AD723295

AFML-TR-71-30

MATERIALS PROCESSING OF RARE EARTH COBALT (RECo$_5$) PERMANENT MAGNETS

P. J. JORGENSEN

Stanford Research Institute
Menlo Park, California 94025
(415) 326-6200, Ext. 4682

SEMIANNUAL INTERIM TECHNICAL REPORT AFML-TR-71-30

JULY 1 TO DECEMBER 31, 1970

D D C

MAY 17 1971

B

39

NOTICE

When Government drawings, specifications, or other data are used for any purpose other than in connection with a definitely related Government procurement operation, the United States Government thereby incurs no responsibility nor any obligation whatsoever; and the fact that the government may have formulated, furnished, or in any way supplied the said drawings, specifications, or other data, is not to be regarded by implication or otherwise as in any manner licensing the holder or any other person or corporation, or conveying any rights or permission to manufacture, use, or sell any patented invention that may in any way be related thereto.

Copies of this report should not be returned unless return is required by security considerations, contractual obligations, or notice on a specific document.

DOCUMENT CONTROL DATA - R & D

(Security classification of title, body of abstract and indexing annotation must be entered when the overall report is classified)

1. ORIGINATING ACTIVITY *(Corporate author)*	2a. REPORT SECURITY CLASSIFICATION
Stanford Research Institute 333 Ravenswood Avenue Menlo Park, California 94025	Unclassified
	2b. GROUP

3 REPORT TITLE

MATERIALS PROCESSING OF RARE EARTH COBALT (RECo$_5$) PERMANENT MAGNETS

4. DESCRIPTIVE NOTES *(Type of report and inclusive dates)*
Semi-Annual Interim Technical Report   July 1 to December 31, 1970

5. AUTHOR(S) *(First name, middle initial, last name)*

Paul J. Jorgensen

6. REPORT DATE	7a. TOTAL NO. OF PAGES	7b. NO. OF REFS
July 1 to December 30, 1970	37	4

8a. CONTRACT OR GRANT NO.	9a. ORIGINATOR'S REPORT NUMBER(S)
F33615-70-C-1624	PYU-8731
b. PROJECT NO. ARPA Order No. 1617	
c.	9b. OTHER REPORT NO(S) *(Any other numbers that may be assigned this report)*
d.	AFML-TR-71-30

10. DISTRIBUTION STATEMENT
This document has been approved for public release and sale;
its distribution is unlimited.

11. SUPPLEMENTARY NOTES	12. SPONSORING MILITARY ACTIVITY
	Air Force Materials Laboratory Wright Patterson Air Force Base Ohio 45433

13. ABSTRACT

Rare earth-cobalt intermetallic compounds show promise for permanent magnets with a higher energy product, BH_{max}, than are currently available. Because fine particles are required for magnetic alignment and sintering, and since the coercivities of these fine particles are sensitive to overgrinding and particle surface preparation, plasma spheroidization and electrodeposition are being investigated as alternative methods for producing strain-free particles. (U)

Apparatus for arc jet plasma spheroidization of particles in argon free of oxygen was constructed and solid spherical particles of SmCo$_5$ and MMCo$_5$ in a size range below 10 μm were produced. Preferential vaporization of samarium causes a reduction in the samarium content of the spherical particles compared with the feed material and causes the formation of a samarium rich fume. (U)

Preliminary fused salt experiments were initiated with the goal of developing methods for electrodeposition of rare earth-cobalt particles. (U)

DD FORM 1473
1 NOV 65

14. KEY WORDS	LINK A		LINK B		LINK C	
	ROLE	WT	ROLE	WT	ROLE	WT
Magnetic Particles						
Rare Earth						
Cobalt						
Plasma Spheroidization						
Electrodeposition						

AFML-TR-71-30

MATERIALS PROCESSING OF RARE EARTH COBALT (RECo$_5$) PERMANENT MAGNETS

P. J. JORGENSEN

The views and conclusions contained in this document are those of the authors and should not be interpreted as necessarily representing the official policies, either expressed or implied, of the Advanced Research Projects Agency or the U. S. Government.
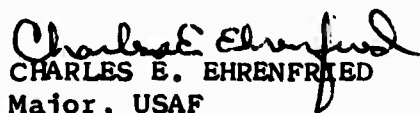
This document has been approved for public release and sale; its distribution is unlimited

FOREWORD

This is the first semiannual interim technical report of the
research program, "Materials Processing of Rare Earth-Cobalt-
Permanent Magnets" under Contract F33615-70-C-1624. Stanford
Research Institute project number is PYU-8731. This project is
being conducted by the Materials Laboratory of Stanford Research
Institute. Dr. Paul J. Jorgensen, Manager of the Ceramics Group,
is the project supervisor. Dr. Robert W. Bartlett of Stanford
University is project consultant.

This report covers research conducted between July 1, 1970 and
December 31, 1970.

This technical report has been reviewed and is approved.

CHARLES E. EHRENFRIED
Major, USAF
Chief, Electromagnetic Materials Branch
Materials Physics Division
Air Force Materials Laboratory

ii

ABSTRACT

Rare earth-cobalt intermetallic compounds show promise for permanent magnets with a higher energy product, BH_{max}, than are currently available. Because fine particles are required for magnetic alignment and sintering, and since the coercivities of these fine particles are sensitive to over-grinding and particle surface preparation, plasma spheroidization and electrodeposition are being investigated as alternative methods for producing strain-free particles.

Apparatus for arc jet plasma spheroidization of particles in argon free of oxygen was constructed and solid spherical particles of $SmCo_5$ and $MMCo_5$ in a size range below 10 μm were produced. Preferential vaporization of samarium causes a reduction in the samarium content of the spherical particles compared with the feed material and causes the formation of a samarium rich fume.

Preliminary fused salt experiments were initiated with the goal of developing methods for electrodeposition of rare earth-cobalt particles.

CONTENTS

ILLUSTRATIONS

I   INTRODUCTION

The $RECo_5$ intermetallic compounds, where RE stands for one of the light rare earths, show a high magnetic saturation and very high magneto-crystalline anisotropy. These properties make them extremely promising materials for fabricating permanent magnets from fine particles by powder pressing and sintering techniques. Although these materials show attractive magnetic properties, coercivities of fine particles have usually been far short of their theoretical potential and are extremely sensitive to overgrinding and particle surface preparation. Free $RECo_5$ magnetic particles have previously been produced only by comminuting arc melted alloys, and these peritectically formed particles exhibit considerable x-ray line broadening and lattice strain. Nucleation of new magnetic domains in particles probably occurs at surfaces, and significant increases in coercivities have occurred after partial dissolution of the particle, removing highly strained surface material.

The objectives of the present program are to investigate alternative materials processing techniques to grinding. The developed techniques are expected to reduce particle imperfections and strain and, consequently, yield higher coercivities.

Two general techniques for the production of fine $RECo_5$ particles are being emphasized: (1) spheroidization--melting and quenching previ-ously comminuted particles dispersed in an inert gas plasma, and (2) electro-deposition of $RECo_5$ particles at temperatures below the $RECo_5$ peritectic. The program has been divided into two tasks for the two materials process-ing techniques, and a third task will cover materials evaluation.

The primary material used in this study is $SmCo_5$, but to provide greater insight into the general potential of each process studied, misch metal cobalt ($MMCo_5$) has also been processed, and $PrCo_5$, YCo_5, and $CeCo_5$ will be processed and evaluated in the future.

1

II   EXPERIMENTAL PROCEDURE

A.   Preparation of Materials for Processing

Preparation of materials for subsequent plasma spheroidization or electrodeposition will consist of the following steps: (1) alloy melting, (2) optional annealing at $1100^{O}C$ in argon, (3) hand crushing, (4) phase identification of sample lots by x-ray diffraction, (5) grinding, and (6) particle size classification by sieving. The last two steps are not required for electrodeposition, since coarse particles will be used, at least initially, for anode materials.

All starting materials are made by melting 99.99% cobalt and the purest available form of the rare earth (e.g., distilled samarium) in a copper hearth arc furnace with a tungsten electrode. Two successive evacuations followed by dry helium backflushes precede melting to prevent contamination. Melting of the rare earth alloy is conducted in a helium pressure near one atmosphere after first melting a titanium ingot getter.

A large number of cobalt-samarium alloy buttons have been made and 100-gram $SmCo_5$ buttons are being produced routinely. Because of preferential samarium volatilization during plasma spheroidization, Sm-Co ingots rich in samarium are being processed.

To assist in the identification of Sm-Co phases and determine the approximate amounts of each phase present, the lattice constants of Buschow and Van der Goot[1] were used to compute lattice spacings, d_0, for various Miller indices. These have been coupled with relative intensities empirically determined, using a diffractometer on powder samples from arc melted alloys to provide identification tables for $SmCo_5$ and Sm_2Co_7, which are shown in Tables 1 and 2. Similar data for Sm_2Co_{17} are available in work by Ostertag and Strnat.[2]

---

[1]K. H. J. Buschow and A. S. Van der Goot, J. Less Common Metals, 14, p. 323 (1968)

[2]W. Ostertag and K. J. Strnat, Acta Cryst., 21, p. 560 (1966)

Table I

X-RAY DIFFRACTION DATA FOR $SmCo_5$

a_o = 5.002

C_o = 3.964

Hexagonal, P6 mm
$CaZn_5$ Type

d_o	hkl	$\%(I/I_o)$	$2\theta(CrK\alpha)$
4.332	100	2	30.67
3.964	001	7	33.59
2.924	101	64	46.12
2.501	110	53	54.52
2.166	200	51	63.86
2.115	111	100	65.58
1.982	002	18	70.61
1.901	201	10	74.11

Table II

X-RAY DIFFRACTION DATA FOR Sm_2Co_7

a_o = 5.041

C_o = 24.327

Hexagonal, $P6_3/mmc$

Ce_2Ni_7 Type

d_o	hkl	%(I/I_o)	$2\theta(CrK\alpha)$
4.366	100	19	30.42
4.055	006	31	32.82
3.845	103	12	34.66
3.546	104	12	37.69
3.047	008	19	44.17
2.971	106	12	45.36
2.719	107	31	49.83
2.521	110	50	54.06
2.495	108	(overlapped with $SmCo_5$ (110))	54.65
2.468	112	6	55.31
2.433	0·0·10	12	57.81
2.328	114	18	58.94
2.298	109	18	59.79
2.183	200	38	63.30
2.174	201	38	63.58
2.148	202	(overlapped with Sm_2Co_7 (116))	64.44
2.141	116	100	64.70
2.125	1·0·10	19	65.23
2.108	203	25	65.84
2.054	204	50	67.77
2.027	0·0·12	100	68.80

Table II (concluded)

d_o	hkl	%(I/I_o)	$2\theta(\text{CrK}\alpha)$
1.992	205	(overlapped with $SmCo_5$ (002))	70.22
1.940	118	12	72.35
1.922	206	6	73.16
1.848	207	16	76.59
1.773	208	16	80.48

Attrition grinding in a Trost jet mill was employed to produce the initial lots of powder. This method required excessive grinding times, and is therefore no longer used. Since the particles will eventually be melted and spheroidized, the final results are not expected to be sensitive to the grinding method, provided contamination is prevented. Ceramic ball mills filled with hexane are currently used for comminution of the intermetallic ingots. The hexane is stored in contact with sodium and the ball mills are loaded in an argon-filled glove box to deter oxidation during grinding.

Particle size versus milling time data have been obtained for $SmCo_5$, $PrCo_5$, and $MMCo_5$.

B.   Plasma Spheroidization

Quenching liquid droplets in an inert atmosphere is usually a simple and effective method for generating fine spherical particles. The liquidus temperatures of the rare earth-cobalt materials of interest are near $1200^{o}C$, which is not an excessive temperature for metal spheroidization. Arc plasma or induction plasma heating avoids the problem of contamination, which results when chemical flame heating is employed, and particles suspended in a plasma can be melted and quenched without agglomeration. Heat transfer to the particles is rapid because of the high plasma temperatures. Although it is comparatively easy to melt $SmCo_5$ in a plasma environment, the high vapor pressure of samarium causes much of it to be vaporized from the droplet. Nevertheless, the possible advantages of fine spherical rare earth-cobalt particles free of comminution-stress-induced imperfections and jagged edges, which are probable sources of magnetic domain nucleation, justifies a serious attempt to produce rare earth-cobalt particles by this method.

The upper spherical particle size limit attained in plasma spheroidization depends upon the sensible heat at the melting point of the material being melted, surface tension, and specific gravity of the particles.[1] For the $RECo_5$ intermetallic compounds it appears that there will be no upper particle size limitation within the size range of

6

interest for fabricating permanent magnets. If a dilute concentration
of solid particles is maintained in the plasma and in the inert gas,
agglomeration can be avoided. The size of spherical particles pro-
duced is controlled by the particle size of the feed, and the lower
size limit depends either on vaporization of the particles or on the
minimum size of the particle agglomerates that can be dispersed
efficiently in the plasma stream. $RECo_5$ particles agglomerate magnet-
ically and this causes added difficulties in achieving efficient
particle dispersions.

An arc jet plasma is being used for the present spheroidization
studies. The primary apparatus consists of a Thermodynamics F-40 arc
jet spheroidization nozzle, a 4-foot-high quenching chamber, and a
40-kilowatt power supply, shown in Fig. 1. Auxiliary equipment has
been added to feed the powder, disperse the particles, collect particles
after spheroidization, and prevent gaseous contamination. A schematic
drawing of the entire apparatus as initially constituted is shown in
Fig. 2. Previously comminuted $RECo_5$ powders were transferred from a
glove box in a sealed bottle and attached to the particle feeder.
Argon that had been purified over a calcium getter was used as a
carrier gas to transmit the particles through the particle feeder and
disperser into the plasma. A second calcium-gettered argon supply was
used for the primary plasma torch gas.

A number of modifications to the apparatus have been made during
this investigation. These include modifications of the particle feeder,
particle dispenser, and particle collection system. Initially, a
Syntron laboratory particle feeder was employed in conjunction with a
high speed turbine particle disperser. The particle feeder was an
all-glass system which allowed transfer without contamination. Solid
particles were discharged near a hot titanium getter and dropped through
a stainless steel bellows into a stainless steel turbine disperser,
which was operated at temperatures above the Curie point of $SmCo_5$.

The initial disperser consisted of a stainless steel housing with
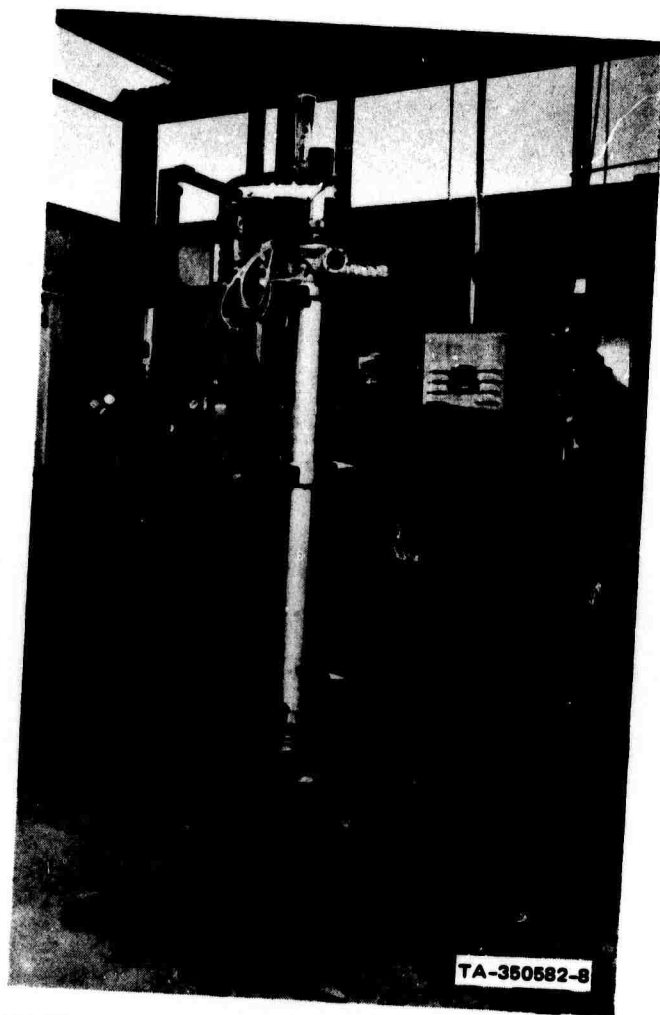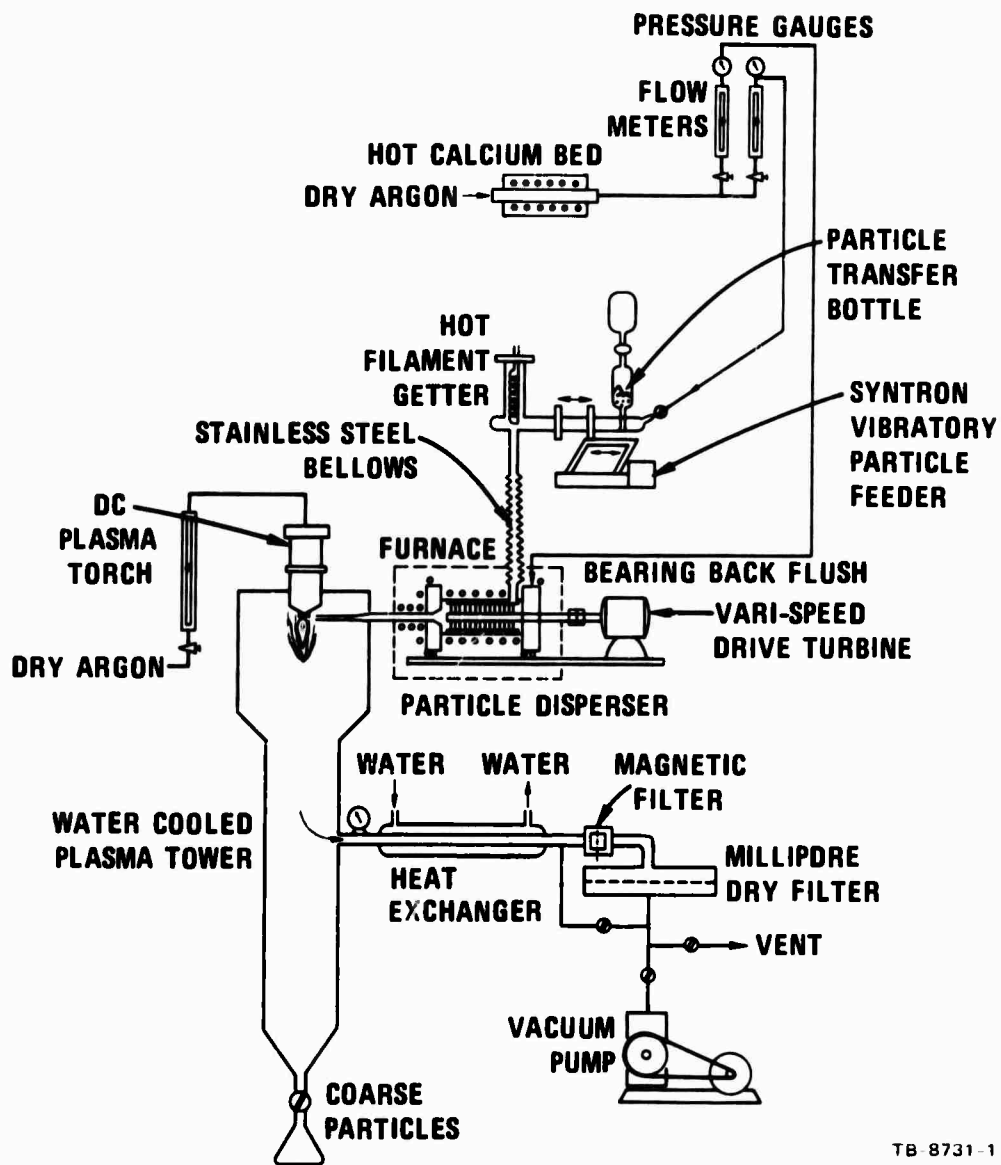ultrahigh vacuum sealed flanges. A stainless steel turbine rotated

7

FIGURE 1   PRIMARY ARC JET PLASMA APPARATUS

FIGURE 2   SKETCH OF PLASMA SPHEROIDIZATION APPARATUS, INITIAL
CONFIGURATION

inside with its drive shaft passing through a boron nitride bearing seal. As particles passed through the disperser, they were heated and impinged by the rotating turbine blades to disengage agglomerates. The discharging particles passed through a short, straight tube into the plasma. The entire disperser was enclosed in an oven located adjacent to the plasma spheroidization chamber.

There were some operational difficulties with this first disperser and during a period when the stainless steel turbine disperser was being modified, a simpler jet disperser was employed on a trial basis. This disperser, shown in Fig. 3, consists of a conical section with steeply sloping walls into which particles are discharged by the particle feeder. An orifice located at right angles to the falling particles causes a high velocity stream of gettered argon to impinge on the particles, dispersing the particles and sweeping them out of the disperser into the plasma. This disperser was also closely coupled to the plasma spheroidization chamber so that a minimum amount of reagglomeration would occur between the disperser and the plasma. The jet disperser was constructed from Lucite, initially as a prototype, to facilitate viewing the particles while they were being dispersed. A stainless steel jet disperser that could be operated above the Curie temperature of $SmCo_5$ was to be constructed later following the results of the Lucite disperser. However, comparisons of the particle size distribution fed to the Lucite jet disperser with the particle size distribution in the plasma spheroidized product indicated that adequate spheroidization was occurring with room temperature dispersion in the Lucite jet disperser. Elaborate precautions to disperse particles above the Curie temperature and prevent cooling below the Curie temperature before injection into the plasma are therefore not required.

Because of its operational simplicity and reliability, the jet dis- perser is now being used. However, it was more convenient to alter the particle feeder from a vibratory type to a variable feed, positive- screw feeder.
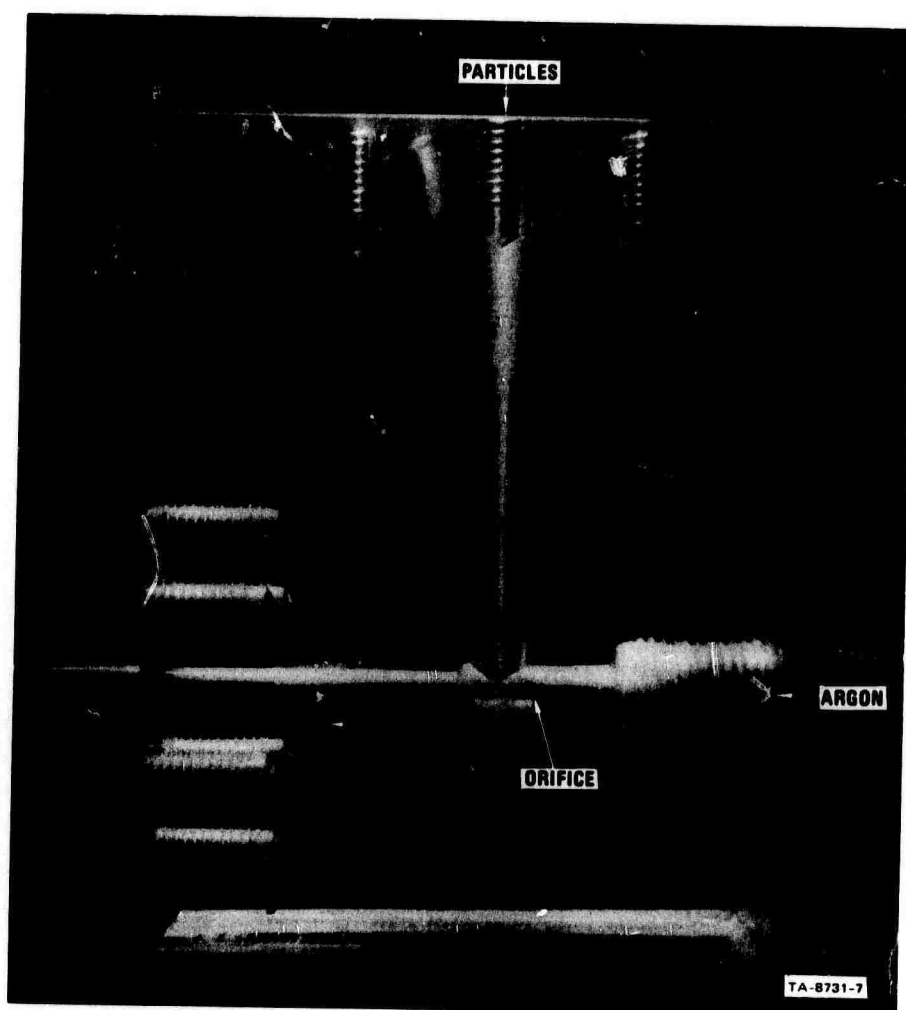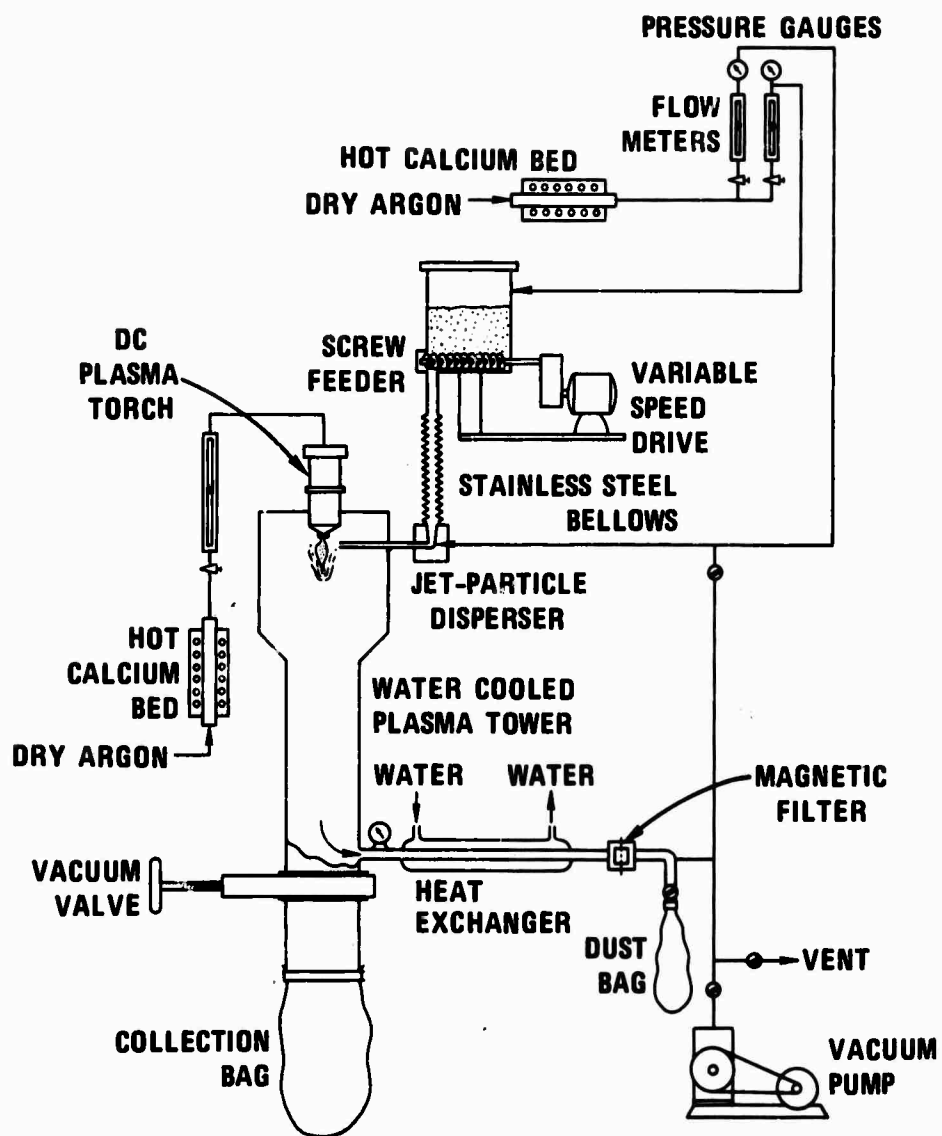
FIGURE 3   ARGON JET PARTICLE DISPERSER

The particle collection system consists of a heat exchanger to cool the effluent argon stream, a magnetic cyclone to collect most of the particles discharging in the stream, and a dust filter. Both paper filters and bags have been used. However, when using feed of approximately 5-micron particle size, over 90% of the spheroidized particles adhered to the walls of the plasma spheroidization chamber. This material was difficult to remove without air contamination, and introduction of air into the system resulted in combustion of the finer particles. Consequently, the spheroidization chamber itself has been modified to operate similarly to a glove box. At the bottom of the spheroidization chamber a large vacuum valve and glove are attached. During spheroidization the valve is closed and the effluent gas is discharged through the exit port located above the vacuum valve. The glove contains gettered argon and, after completion of a run, the valve is opened so that the glove can be used to dislodge particles from the spheroidization chamber while it is still sealed from the ambient atmosphere. The spheroidized particles are removed with a small brush and concentrated on the glove below the vacuum valve. The vacuum valve is then closed and the entire assembly including the vacuum valve is removed from the spheroidization chamber and taken to a glove box where it is opened and the particles are removed. A schematic drawing of the plasma spheroidization apparatus as it is now constituted is shown in Fig. 4.

C. Evaluation of Processed Materials

The evaluation of cobalt-rare earth particles falls into three broad categories: (1) chemical analysis and phase identification, (2) particle size analysis, and (3) magnetic property evaluation. The major source of chemical contamination is from gaseous impurities introduced during processing. Arrangements have been made for neutron activation analysis of oxygen at Gulf Radiation Laboratories in San Diego, California. Phase identification is being made with the Norelco x-ray diffractometer using either chromium or cobalt radiation. Particle sizes are being determined by sieving, optical microscopy of particles

12

PRESSURE GAUGES

FLOW METERS

HOT CALCIUM BED
DRY ARGON

DC PLASMA TORCH

SCREW FEEDER

VARIABLE SPEED DRIVE

STAINLESS STEEL BELLOWS

JET-PARTICLE DISPERSER

HOT CALCIUM BED

DRY ARGON

WATER COOLED PLASMA TOWER

WATER   WATER

MAGNETIC FILTER

VACUUM VALVE

HEAT EXCHANGER

DUST BAG

VENT

COLLECTION BAG

VACUUM PUMP

TA-8731-6

FIGURE 4   SKETCH OF PLASMA SPHEROIDIZATION, PRESENT CONFIGURATION

13

spread on a microscope slide, and scanning electron microscopy; average particle size is being determined by Fisher subsieve analysis.

Techniques have been developed and implemented to impregnate rare earth-cobalt particles in an epoxy matrix that is injected into a 5/16-inch x 11/16-inch standard pharmaceutical capsule for magnetic evaluation. The capsules are loaded and covered in a glove box and then transferred out of the glove box to an alignment jig inserted between the poles of a Varian V-4004 electromagnet. The particles are aligned in a 10,000-Oersted field while the samples are heated to 80°C in the alignment jig and partial curing of the epoxy occurs. Six sample capsules can be aligned simultaneously.

Since coercivities obtained with $SmCo_5$ powders usually increase with the previous magnetizing field,[3] the initial plans to measure hysteresis loops using a 25-kilo-Oersted magnet at the Institute have been abandoned. Components for a 100-kilo-Oersted vibrating-sample magnetometer system have been ordered. The magnetometer has been received but 3 months of delays in producing the superconducting magnetic coils have caused a delay in receiving the superconducting field magnet. The remaining components for this system are not expected before March 1, 1971. Nevertheless, this equipment should be operational shortly thereafter and provide excellent magnetic evaluation capability. The magnetometer is designed to provide a 1-inch uniform-field sample chamber and permit sample measurements from cryogenic to room temperatures.

[3] J. J. Becker, "Technology Development for Transition Metal-Rare Earth High-Performance Magnetic Materials," Monthly Status Report, August 1970

14

III EXPERIMENTAL RESULTS

A.   Plasma Spheroidization

Plasma spheroidization runs have been made on mischmetal cobalt
($MMCo_5$) and $SmCo_5$. Most of the comminuted particles can be sieved through
a -20 μm nylon screen using the magnetic brush technique developed by
Becker et al.[4] and the average particle size as determined by Fisher Anal-
ysis has been 2 to 3 μm. The particle sizes of these feed materials have
probably been somewhat smaller than usually employed by other investigators
in fabricating optimum $SmCo_5$ magnets, since the measured coercivity begins
to drop as the comminuted particle size becomes smaller than about 4 μm.

All of the experiments conducted to date have been at a uniform
power setting of 15 kilowatts and a uniform argon flow rate, with introduc-
tion of the particles into the plasma at the same elevation in the plasma
column.

The results of these experiments may be summarized as follows:
(1) all of the particles are spheroidized and solid spheres rather than
hollow spheres are formed, (2) the particle size distribution of the
spheres is essentially the same as the particle size distribution of the
feed, as evidenced by optical and scanning electron microscopy, (3) there
is a slight vaporization loss from the $MMCo_5$ particles and a substantial
loss of samarium by vaporization from the $SmCo_5$ particles, and (4) the
vapor recondenses in the form of a very fine fume which is collected with
the spherical particles.

Scanning electron micrographs of the initial particles and the
spheroidized particles from a $MMCo_5$ run and a $SmCo_5$ run are shown in
Figs. 5 and 6, respectively. All of these micrographs were taken at the
same magnification and are typical of the starting feed and spheroidized

---

[4] J. J. Becker, et al., Summary Technical Report, AFML-TR-68-54, "Research
to Investigate Fundamental Magnetic Interactions in Selected Materials,"
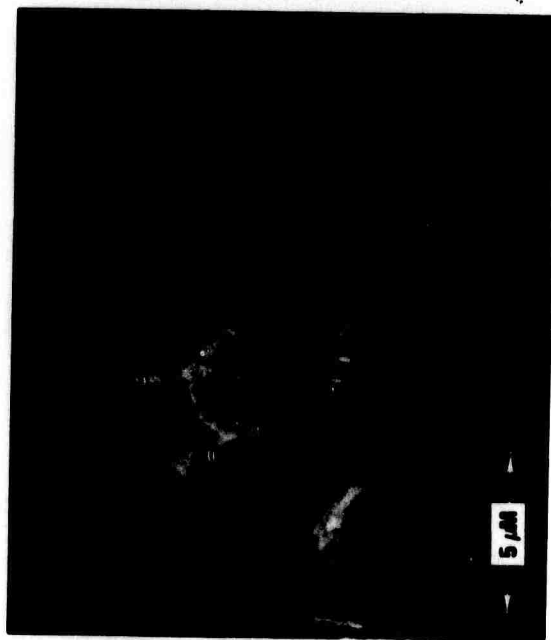GE Research & Development Center, p. 8, April 1968

SPHERDIDIZED
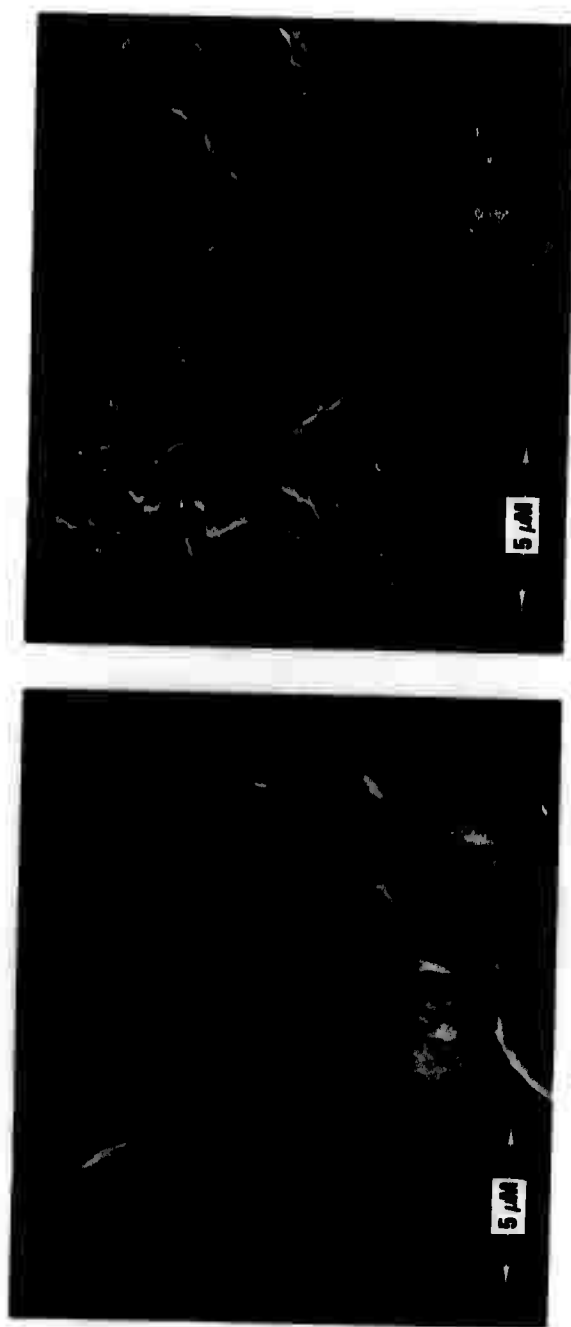
COMMINUTED

TA-8731-8

FIGURE 5   SCANNING ELECTRON MICROGRAPHS BEFORE AND AFTER PLASMA
SPHEROIDIZATION OF MMCo$_5$

16

SPHERDIDIZED

COMMINUTED

TA-8731-9

FIGURE 6   SCANNING ELECTRON MICROGRAPHS BEFORE AND AFTER PLASMA
SPHEROIDIZATION OF SmCo$_5$

17

powder. Many jagged edges and reentrant angles can be seen on the
starting feed particles and the general morphology is fairly typical
of fractured brittle solids. Scanning electron micrographs of comminuted
particles were similar for grinding in the Trost mill or by ball milling.

The micrographs of the spheroidized particles show a bimodal size
distribution of (1) larger spherical particles and (2) extremely fine
(submicron) fume. Note that there is substantially more fume in the
micrograph of the samarium-cobalt spheroidized particle than in the
micrograph at the spheroidized mischmetal-cobalt particles, and this
is a typical result for these two materials. A more direct comparison
of the extra fume surrounding the $SmCo_5$ spherical particle with that
around the $MMCo_5$ spherical particle is shown in Fig. 7, which consists
of two scanning electron micrographs at somewhat higher magnification
than shown in the previous figures. Although fume is found separate
from spherical particles, some fume also attaches to the particles and
the attachment appears to be strong enough to suggest magnetic agglo-
meration of fume and particles. A magnetic interaction would require
that the fume contain cobalt as well as samarium or other volatile
rare earths. This was confirmed by electron microprobe analyses of
the $SmCo_5$ spheroidization products. Powders were mounted in a conducting
mount, sectioned and polished for metallographic and microprobe analysis.
The samarium content of the spherical particles varied considerably,
from 10 to 35 wt% with an average Sm content below the stoichiometric
amount for $SmCo_5$. The balance of the material in the spherical parti-
cles was cobalt, and microprobe spectroanalysis showed that the impurity
content of the spherical particles was identical with the impurity
content of the starting materials--showing very minor amounts of silicon,
aluminum, and cerium.

The fume did contain both samarium and cobalt but the samarium-
cobalt ratio was higher than that obtained with the spherical particles.
Because of the low effective density of a mass of fume particles it is
not possible to make a quantitative analysis of these particles based

18

FIGURE 7   SPHERICAL PARTICLES AND FUME AFTER PLASMA SPHEROIDIZATION
OF RECo$_5$

19

on relative intensities of samarium, cobalt, and other elements. However, the major constituents were cobalt, samarium, and oxygen. The oxygen was introduced when the system was opened to air and some chemical reaction occurred with a noticeable release of heat. Impurities found in the starting materials and the spherical particles were also present in the fume.

The electron microprobe fluorescent analyses of spherical particles and fume found in the $SmCo_5$ are summarized in Table 3. Average particle size analyses of spheroidized products measured by the Fisher method were in the range from 0.3 to 0.7 μm. The average size is lowered from the average size of the starting material only by the presence of the fume. These results are entirely consistent with melting coupled with substantial vaporization of the rare earth followed by quenching of both the spherical particles and fume.

The x-ray diffraction patterns of $SmCo_5$ after spheroidization show a few of the major $SmCo_5$ diffraction peaks with considerable broadening and lowering of intensity. A single strong peak characteristic of cobalt also appears. These x-ray diffraction patterns are fairly ambiguous. Although to some extent they suggest a cobalt shell surrounding a $SmCo_5$ core, sectioned and polished spherical particles appear to be single phase. The spherical particles are continuous solids rather than hollow spheres as often results from spheroidization of metals, see Fig. 8. The spherical particles are weakly magnetic and examination under polarized light indicates multimagnetic domain particles.

$SmCo_5$ starting powders and the resulting spheroidized powders have been encapsulated in an epoxy matrix and aligned in a field (10,000 Oe). Although these materials have not been magnetically saturated and no magnetic measurements have been made, the capsules with spheroidized material are more weakly magnetic than the starting comminuted material. This is not surprising, since the spheroidized material is far removed from the stoichiometric $SmCo_5$ composition. Any utility from spheroidizing particles cannot be determined until spherical particles of stoichiometric $SmCo_5$ are produced. This is the goal of future experiments.

20

Table III

SEMI-QUANTITATIVE ANALYSIS

OF INITIAL AND SPHEROIDIZED $SmCo_5$ - Run 7

(Weight Percent)

	Co	Sm	Al	Si	Ce	La	O_2	C
Initial	61.0 [1,2]	31.6 [1]	~0.2	~0.2	~0.3	<0.1	Nil	-
Spherical particles	60-85 (Avg.=68%)	12-35 (Avg.=28%)	~0.3	~0.3	~0.3	<0.1	Nil	-
Fume	22-31 (Avg.=27%)	31-36 (Avg.=33%)	~0.2	~0.4	~0.3	<0.1	~12 [3,4] (uncorr.)	~5 [4] (uncorr.)

[1] The cobalt and samarium feed analyses of individual particles varied ±2%.

[2] Stoichiometric $SmCo_5$ contains 33.8% Sm and 66.2% Co.

[3] Oxidation occurred with considerable release of heat when air was admitted to the sample.

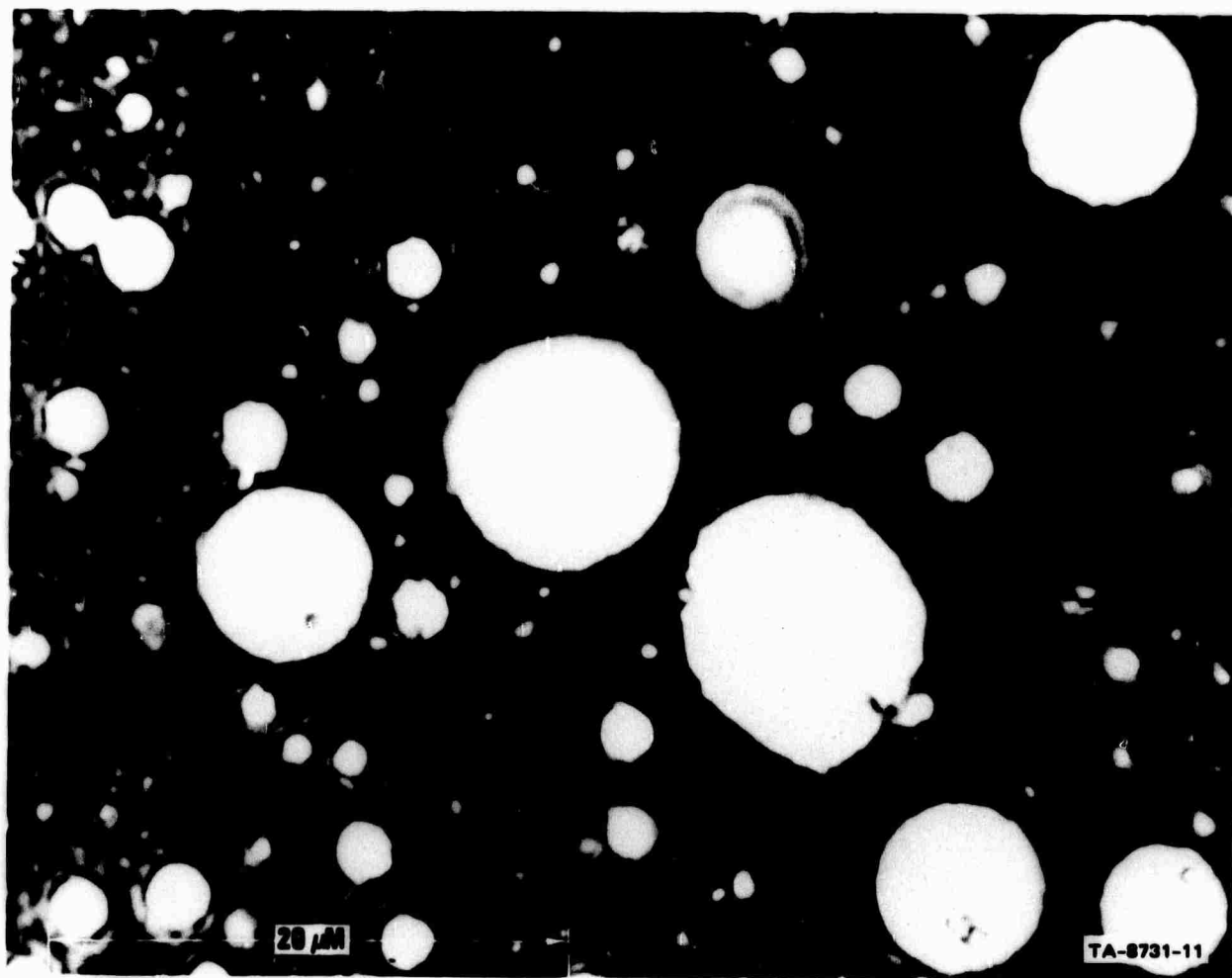[4] Based on relative intensities without absorption or other matrix corrections.

21

FIGURE 8   SPHEROIDIZED SmCo₅ IN SECTION (BRIGHT FIELD)

22

B. Electrodeposition

Several of the $RECo_5$ compounds, including the $SmCo_5$, do not melt congruently. When these materials are produced by cooling the liquid of this composition, RE_2Co_{17} is crystallized and on further cooling a peritectic reaction between the residual samarium-rich liquid and the RE_2Co_{17} solid compound is required to produce $RECo_5$. A solid state rearrangement is necessary, and it is possible that a homogeneous material will not be obtained. Poor x-ray diffraction patterns from these materials are obtained even without extensive grinding, indicating poor homogeneity and accompanying crystal strain caused by the sluggish peritectic reaction. It is highly desirable to explore the magnetic properties of $RECo_5$ particles produced at temperatures below the peritectic temperature. In principle, this can be accomplished by growing crystals of the $RECo_5$ compound from a suitable solvent for both the rare earth and cobalt.

Electrodeposition from fused fluorides is currently being investigated and studies on organic electrolytes are planned next quarter. The morphology of a crystal deposit grown from solution depends on many factors, but the production of whiskers or powder requires low concentrations of the solute such that diffusion in the liquid controls the crystal growth kinetics.

Several materials compatibility experiments were made with a eutectic mixture of BaF_2 and LiF at 950°C. These fluorides are the most stable within the alkaline earth and alkali metal groups. Thermodynamic calculations indicate that this salt mixture should be relatively stable with respect to exchange between samarium and barium or lithium. Some samarium might be replaced by barium but the resulting formation of samarium fluoride should be less than 1% of the salt.

Many metals are known to dissolve in their own fused halides. For example, fused nickel chloride will dissolve nickel metal but not other metals. The amount of nickel dissolved is about 10% by weight. Dissolution of excess samarium in its fluoride is also known

23

to occur but its solubility in the BaF_2-LiF mixture was not expected.
A crucible test showed that large amounts of samarium were dissolved
in the BaF_2-LiF mixture and that a fine precipitate with a metallic
luster was formed. The metallic precipitate was easily oxidized,
suggesting that the precipitate was samarium metal. This was later
confirmed by electron microprobe examinations of the cooled salt.

Figure 9 shows two images of a typical particle dispersed in the
salt. The left image shows the secondary electron image of the surface,
while the right image is the samarium, $L\alpha_1$, characteristic x-ray image.
Intensity counts for samarium and barium were taken on several particles
and within the salt matrix. A trace of samarium remained in solution,
probably as samarium ions, and a small amount of barium was reduced by
the samarium. The estimated samarium content of the salt at room temper-
ature was less than 2%. The reduced barium was usually present as a small
barium-samarium alloy particle core surrounded by more metallic samarium.
This indicates that barium is more easily rejected than samarium from the
fused salt solution at higher temperatures. Except for the occasional
barium-rich cores the metallic particles were entirely samarium.

It is clear from these analyses that a small amount of samarium
exchanges with barium in barium fluoride and that the amount of exchange,
approximately 2%, agrees reasonably well with thermodynamic data.
It is also clear that large amounts of samarium are dissolved in the
fused salt, without oxidation to a higher valence state, and subsequently
reprecipitated as metallic samarium particles on cooling.

Electrodeposition of samarium will therefore require saturation
of the electrolyte with excess samarium metal. If this is not done,
samarium deposited at the cathode would redissolve in the electrolyte.
When samarium dissolution tests were made in graphite crucibles, the
dissolved samarium migrated to the graphite crucible walls and reacted
to form samarium carbide. Fortunately, molybdenum does not react
with samarium or the fused salts and is sufficiently refractory to
make a suitable crucible material. Fused salt compatibility tests

24
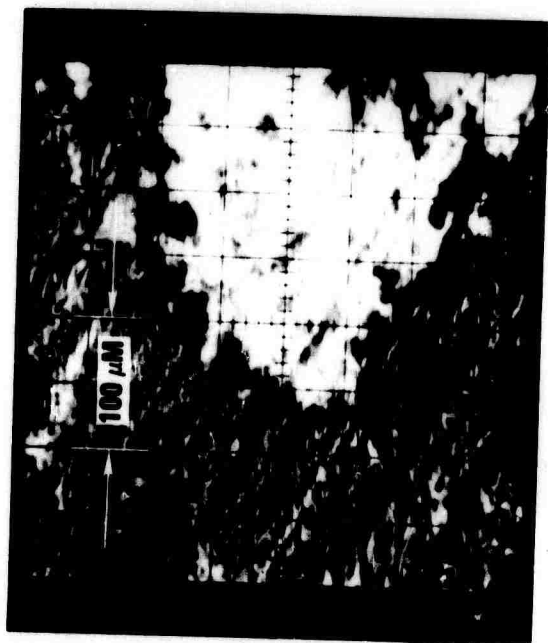
SECONDARY ELECTRON IMAGE
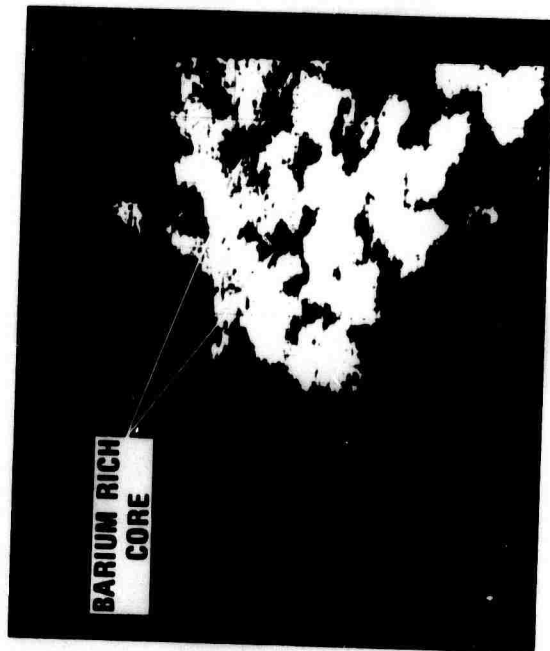
SAMARIUM L α_1 X-RAY IMAGE

TA-8731-12

FIGURE 9   MICROPROBE IMAGES OF SAMARIUM PARTICLE REPRECIPITATED IN BaF_2-LiF SALT
MIXTURE (25 KVA BEAM)

25

made with cobalt, $SmCo_5$, and $MMCo_5$, using the barium fluoride-lithium fluoride electrolyte at 950°C showed that there was no dissolution of these metals and alloys in the electrolyte.

C. Solution Growth of $SmCo_5$

Three solution transport experiments were made using molten zinc. These experiments were designed to dissolve $SmCo_5$ in the hotter zone of the experiment chamber and to transport both cobalt and samarium within the zinc solvent to the cooler zone of the chamber, where reprecipitation of the intermetallic compound would occur. In this manner, it was hoped that a large cast ingot of intermetallic compound could be converted to fine particles at temperatures below the peri-tectic temperature. The excess zinc would be removed by evaporation, since the zinc vapor pressure is considerably greater than the samarium vapor pressure. Chemical analyses of particles transported in zinc and subsequently separated by hydrochloric acid leaching of the zinc indicated that the particles were entirely cobalt.

IV SUMMARY

During the first six months of this program, the plasma spheroidization apparatus was redesigned to process rare earth-cobalt materials This involved redesigning and testing of the particle feed system, the particle dispenser, and particle collection system. Improvements such as gettered gas supplies were added to the apparatus in order to spheroidize these materials at extremely low oxygen partial pressures.

Particle dispersion and spheroidization of $SmCo_5$ and $MMCo_5$ materials have been accomplished. The spherical particles are solid rather than hollow spheres, and have a particle size distribution essentially the same as the particle size distribution of the initial particle feed material.

Preferential vaporization of samarium causes the plasma-spheroidized particles to be low in samarium content. Experimental parameters are currently being investigated so that spherical stoichiometric particles of $SmCo_5$ can be obtained. Experiments are also being conducted with $PrCo_5$ because of the lower vapor pressure of praseodymium.

Electrodeposition cells consisting of $SmCo_5$ anodes, molybdenum cathodes, and BaF_2-LiF electrolytes have been designed. Preliminary results indicate that samarium metal can be dissolved in the electrolyte. A small amount (approximately 2%) of the BaF_2 is reduced at $950^{o}C$ by the samarium to produce free barium. $SmCo_5$ and $MMCo_5$ are not dissolved in the BaF_2-LiF electrolyte. Diffusion-limited steady-state conditions are being employed to investigate the growth of small dendritic particles of $SmCo_5$ formed below the peritectic temperature.

Electrodeposition cells using organic electrolytes have also been designed and experimental results will be obtained in the third quarter of the program.

A vibrating magnetometer coupled to a 100 kG superconducting magnet is currently being built and is expected to be in operation during the third quarter so that magnetic properties of the produced materials can be evaluated.

V   FUTURE WORK

Plasma spheroidization runs will be continued with variations in the following parameters to determine their effect on composition of the spherical particles produced: (1) arc plasma power, (2) elevation of particle injection in the plasma column, and, consequently, residence time in the plasma, (3) particle size of the feed, and (4) cobalt-samarium ratio in the feed. Lower power settings, larger particles, shorter residence times, and higher samarium-cobalt ratios should improve the samarium-cobalt ratio in the spherical particles produced. The samarium-cobalt ratio in the feed will be increased by both higher samarium-cobalt ratios in the comminuted alloy and by the use of mixtures of pure samarium and samarium-cobalt alloy particles. An excess of samarium in the feed may cause a sufficient vapor pressure in the plasma to suppress vaporization from the alloy particle.

Methods must also be found to remove excess fume from the spherical particles. Classification using inert gases will be explored. Spheroidization of other $RECo_5$ compounds should be less difficult since samarium has the highest vapor pressure of the rare earths. Plasma spheroidization experiments are planned with $PrCo_5$. Ingots of $SmCo_5$ have been cast in boron nitride crucibles. The work to date has been done with hot pressed boron nitride containing approximately 3% B_2O_3. Pyrolytic boron nitride crucibles have been received and will be used for casting in the future. These cast ingots will be used as anodes in the electrodeposition experiments. The anode will be held with a graphite ring and dipped into the molten electrolyte containing an excess of samarium in the bottom of the molybdenum electrolytic cell. A molybdenum cathode and molybdenum-sheathed thermocouple will be placed in the electrolyte. The electrolytic cell and both of the electrodes can be independently raised and lowered by vertical shafts passing through Wilson seals in the vacuum furnace. A sketch is shown in Fig. 10. The electrodeposition experiments will begin as soon as specially ordered molybdenum electrolytic cells are received.

29
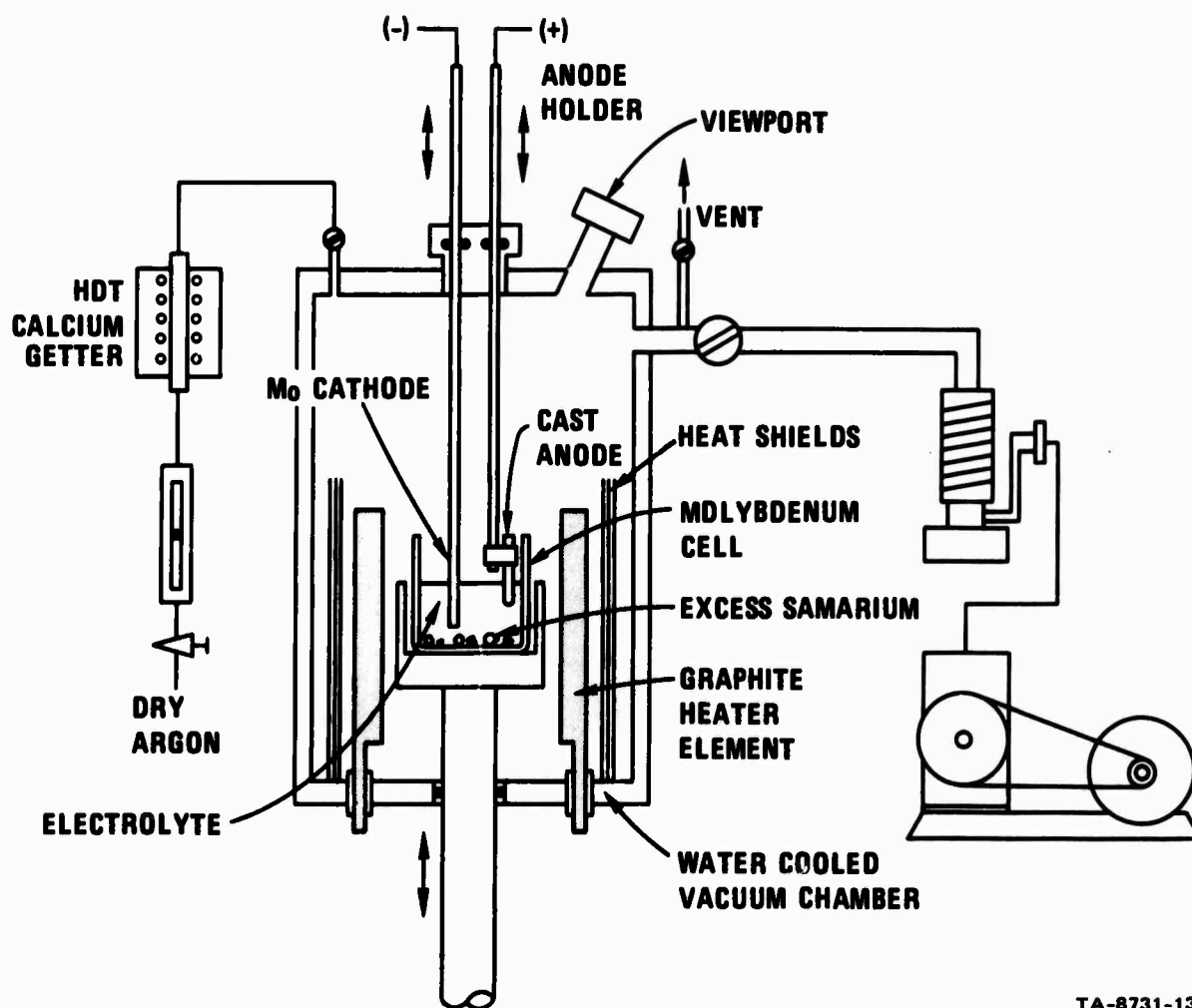
FIGURE 10   SKETCH OF FUSED SALT ELECTROLYTIC CELL

TA-8731-13

30